

Kaluza-Klein Dark Matter: Direct Detection vis-a-vis LHC

Sebastian Arrenberg and Laura Baudis

Department of Physics, University of Zürich, Zürich, 8057, Switzerland

Kyoungchul Kong

Department of Physics and Astronomy, University of Kansas, Lawrence, KS 66045 USA

Konstantin T. Matchev

*Institute for Fundamental Theory, Physics Department,
University of Florida, Gainesville, FL 32611, USA*

Jonghee Yoo

Fermi National Accelerator Laboratory, Batavia, IL 60510, USA and

We present updated results on the complementarity between high-energy colliders and dark matter direct detection experiments in the context of Universal Extra Dimensions (UED). In models with relatively small mass splittings between the dark matter candidate and the rest of the (colored) spectrum, the collider sensitivity is diminished, but direct detection rates are enhanced. UED provide a natural framework to study such mass degeneracies. We discuss the detection prospects for the KK photon γ_1 and the KK Z -boson Z_1 , combining the expected LHC reach with cosmological constraints from WMAP/Planck, and the sensitivity of current or planned direct detection experiments. Allowing for general mass splittings, neither colliders, nor direct detection experiments by themselves can explore all of the relevant KK dark matter parameter space. Nevertheless, they probe different parameter space regions, and the combination of the two types of constraints can be quite powerful.

We present updated results on the complementarity between high-energy colliders and dark matter direct detection experiments [1] in the context of Universal Extra Dimensions [2]. As our reference, we take the mass spectrum in Minimal Universal Extra Dimensions (MUED), which is fixed by the radius (R) of the extra dimension and the cut-off scale (Λ) [3, 4]. To illustrate the complementarity between dark matter detection and searches at the LHC, we introduce a slope in the MUED mass spectrum, in terms of the mass splitting (Δ_{q_1}) between the mass of the lightest Kaluza-Klein (KK) partner (LKP) m_{LKP} and the KK quark mass m_{q_1} :

$$\Delta_{q_1} = \frac{m_{q_1} - m_{LKP}}{m_{LKP}}.$$

We take Δ_{q_1} as a free parameter, which is possible in a more general framework with boundary terms and bulk masses (see, e.g., [5]). The LKP is taken to be either the KK mode γ_1 of the photon (as in MUED), or the KK mode Z_1 of the Z -boson. In the latter case, we assume that the gluon and the remaining particles to be respectively 20% and 10% heavier than the Z_1 . This choice is only made for definiteness, and does not impact our results, as long as the remaining particles are sufficiently heavy and do not participate in co-annihilation processes.

In the so defined (m_{LKP}, Δ_{q_1}) parameter plane, in Fig. 1 we superimpose the limit on the spin-independent elastic scattering cross section, the limit on the relic abundance and the LHC reach in the four leptons plus missing energy ($4\ell + \cancel{E}_T$) channel which has been studied in [3] at the 14 TeV (see Ref. [6] for 7+8 TeV). This signature results from the pair production (direct or indirect)

of $SU(2)_W$ -doublet KK quarks, which subsequently decay to Z_1 's and jets. The leptons (electrons or muons) arise from the $Z_1 \rightarrow \ell^+ \ell^- \gamma_1$ decay, whose branching fraction is approximately $1/3$ [3]. Requiring a 5σ excess at a luminosity of 100 fb^{-1} , the LHC reach extends up to $R^{-1} \approx m_{\gamma_1} \sim 1.5 \text{ TeV}$, which is shown as the right-most boundary of the (yellow) shaded region in Fig. 1a. The slope of that boundary is due to the fact that as Δ_{q_1} increases, so do the KK quark masses, and their production cross sections are correspondingly getting suppressed, diminishing the reach. We account for the loss in cross section according to the results from Ref. [7], assuming also that, as expected, the level-2 KK particles are about two times heavier than those at level 1. Points which are well inside the (yellow) shaded region, of course, would be discovered much earlier at the LHC. Notice, however, that the LHC reach in this channel completely disappears for Δ_{q_1} less than about 8%. This is where the KK quarks become lighter than the Z_1 (recall that in Fig. 1a m_{Z_1} is fixed according to the MUED spectrum) and the $q_1 \rightarrow Z_1$ decays are turned off. Instead, the KK quarks all decay directly to the γ_1 LKP and (relatively soft) jets, presenting a monumental challenge for an LHC discovery. So far there have been no studies of the collider phenomenology of a Z_1 LKP scenario, but it appears to be extremely challenging, especially if the KK quarks are light and decay directly to the LKP. This is why there is no LHC reach shown in Fig. 1b. We draw attention once again to the lack of sensitivity at small Δ_{q_1} : such small mass splittings are quite problematic for collider searches. The current LHC exclusion limit (95% C.L. at 8 TeV) on R^{-1} is about 1250 GeV for $\Lambda R = 20$ [6]. and this is shown as the dotted (cyan) line. The horizontal line at $\Delta_{q_1} \sim 0.2$ is the average mass splitting in MUED. To indicate roughly the approximate boundary of the excluded region, the slanted line around 1 TeV is added, assuming the shape of the boundary is similar to that for the LHC14 reach.

In Fig. 1 we contrast the LHC reach with the relic density constraints [8, 9] and with the sensitivity of direct detection experiments [10, 11]. The green shaded region labelled by 100% represents 2σ band, $0.117 < \Omega_{CDM} h^2 < 0.1204$ [12] and the black solid line inside this band is the central value $\Omega_{CDM} h^2 = 0.1187$. The region above and to the right of this band is disfavored since UED would then predict too much dark matter. The green-shaded region is where KK dark matter is sufficient to explain all of the dark matter in the universe, while in the remaining region to the left of the green band the LKP can make up only a fraction of the dark matter in the universe. We have indicated with the black dotted contours the parameter region where the LKP would contribute only 10% and 1% to the total dark matter budget. Finally, the solid (CDMS [13] in blue and XENON100 [14] in red) lines show the current direct detection limits, while the dotted and dashed lines show projected sensitivities for future experiments [15–17]¹.

Fig. 1 demonstrates the complementarity between the three different types of probes which we are considering. First, the parameter space region at very large m_{LKP} is inconsistent with cosmology – if the dark matter WIMP is too heavy, its relic density is too large. The exact numerical bound on the LKP mass may vary, depending on the particle nature of the WIMP (compare Fig. 1a to Fig. 1b) and the presence or absence of coannihilations (compare the m_{LKP} bound at small Δ_{q_1} to the bound at large Δ_{q_1}). Nevertheless, we can see that, in general, cosmology does provide an upper limit on the WIMP mass. On the other hand, colliders are sensitive to the region of relatively large mass splittings Δ_{q_1} , while direct detection experiments are at their best at small Δ_{q_1} and small m_{LKP} . The relevant parameter space is therefore getting squeezed from opposite directions and is bound to be covered eventually. This is already seen in the case of γ_1 LKP from Fig. 1a: the future experiments push up the current limit almost to the WMAP/Planck

¹ Here and in the rest of the paper, when presenting experimental limits in an under-dense or an over-dense parameter space region, we do not rescale the expected direct detection rates with the calculated relic density. The latter is much more model-dependent, e.g. the mismatch with the relic abundance may be fixed by non-standard cosmological evolution, having no effect on the rest of our analysis.

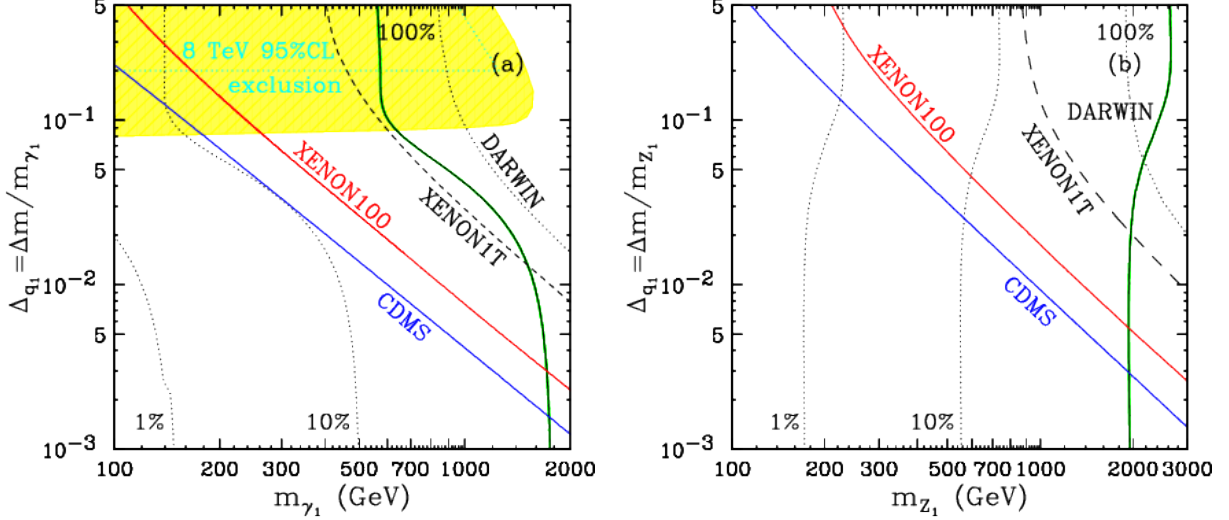


FIG. 1: Combined plot of the direct detection limit on the spin-independent cross section, the limit from the relic abundance and the LHC reach for (a) γ_1 and (b) Z_1 , in the parameter plane of the LKP mass and the mass splitting Δ_{q_1} . The remaining KK masses have been fixed as in Ref. [4] and the SM Higgs mass is $m_h = 125$ GeV. $\Lambda R = 20$ is assumed. The black solid line accounts for all of the dark matter (100%) and the two black dotted lines show 10% and 1%, respectively. The green band shows the WMAP/Planck range, $0.117 < \Omega_{CDM} h^2 < 0.1204$. The blue (red) solid line labelled by CDMS (XENON100) shows the current limit of the experiment whereas the dashed and dotted lines represent projected limits of future experiments. In the case of γ_1 LKP, a ton-scale experiment will rule out most of the parameter space while there is little parameter space left in the case of Z_1 LKP. The yellow region in the case of γ_1 LKP shows parameter space that could be covered by the collider search in the $4\ell + \cancel{E}_T$ channel at the LHC with a luminosity of 100 fb^{-1} [3].

band. In the case of Z_1 LKP the available parameter space is larger and will not be closed with the currently envisioned experiments alone. However, one should keep in mind that detailed LHC studies for that scenario are still lacking.

Similarly the spin-dependent elastic scattering cross sections also exhibit an enhancement at small Δ_{q_1} . In Fig. 2 we combine existing limits from three different experiments (XENON100 [18], SIMPLE [19] and COUPP [20]) in the (m_{LKP}, Δ_{q_1}) plane. Panel (a) (panel (b)) shows the constraints from the WIMP-neutron (WIMP-proton) SD cross sections. The rest of the KK spectrum has been fixed as in Fig. 1. The solid (dashed) curves are limits on γ_1 (Z_1) from each experiment. The constraints from LHC and WMAP on the (m_{LKP}, Δ_{q_1}) parameter space are the same as in Fig. 1.

By comparing Figs. 1 and 2 we see that, as expected, the parameter space constraints for SI interactions are stronger than those for SD interactions. For example, in perhaps the most interesting range of LKP masses from 300 GeV to 1 TeV, the SI limits on Δ_{q_1} in Fig. 1 range from $\sim 10^{-1}$ down to $\sim 10^{-2}$. On the other hand, the SD bounds on Δ_{q_1} for the same range of m_{LKP} are about an order of magnitude smaller (i.e. weaker). We also notice that the constraints for γ_1 LKP are stronger than for Z_1 LKP. This can be easily understood since for the same LKP mass and KK mass splitting, the γ_1 SD cross sections are typically larger.

Fig. 2 also reveals that the experiments rank differently with respect to their SD limits on protons and neutrons. For example, SIMPLE and COUPP are more sensitive to the proton cross section, while XENON100 is more sensitive to the neutron cross section. As a result, the current best SD limit on protons comes from COUPP, but the current best SD limit on neutrons comes from XENON100.

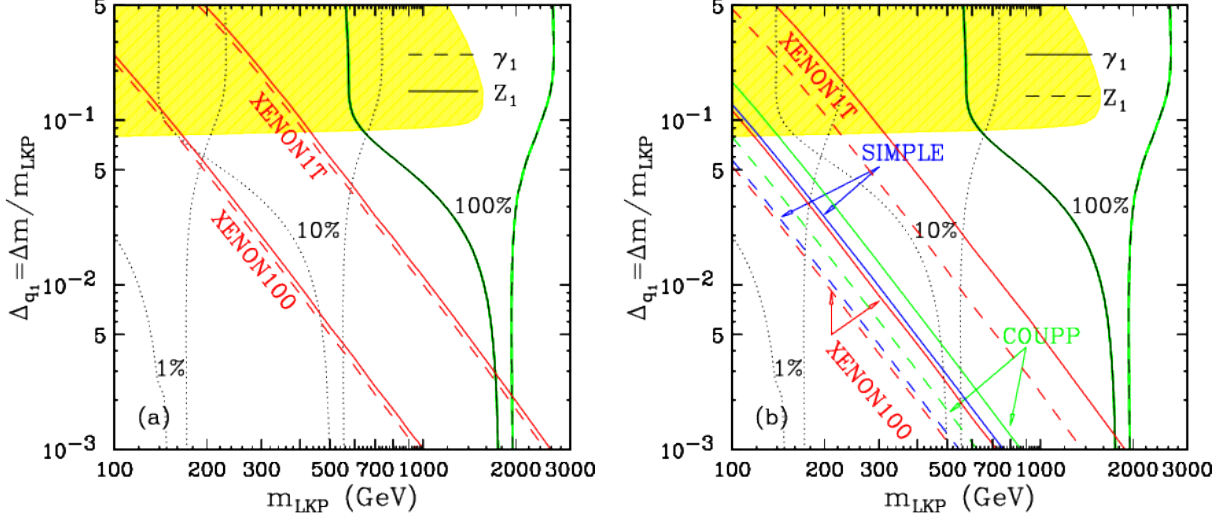


FIG. 2: Experimental upper bounds (90% C.L.) on the spin-dependent elastic scattering cross sections on (a) neutrons and (b) protons in the m_{LKP} - Δ_{q_1} plane. The solid (dashed) curves are limits on γ_1 (Z_1) from each experiment. Shaded regions and dotted lines are defined in the same way as in Fig. 1. The depicted LHC reach (yellow shaded region) applies only to the case of γ_1 LKP.

Acknowledgments

This work is in part supported by the Swiss National Foundation SNF and the U.S. Department of Energy.

-
- [1] S. Arrenberg, L. Baudis, K. Kong, K. T. Matchev and J. Yoo, Phys. Rev. D **78**, 056002 (2008) [arXiv:0805.4210 [hep-ph]].
 - [2] T. Appelquist, H. -C. Cheng and B. A. Dobrescu, Phys. Rev. D **64**, 035002 (2001) [hep-ph/0012100].
 - [3] H. -C. Cheng, K. T. Matchev and M. Schmaltz, Phys. Rev. D **66**, 056006 (2002) [hep-ph/0205314].
 - [4] H. -C. Cheng, K. T. Matchev and M. Schmaltz, Phys. Rev. D **66**, 036005 (2002) [hep-ph/0204342].
 - [5] T. Flacke, K. Kong and S. C. Park, JHEP **1305**, 111 (2013) [arXiv:1303.0872 [hep-ph]].
 - [6] A. Belyaev, M. Brown, J. Moreno and C. Papineau, JHEP **1306**, 080 (2013) [arXiv:1212.4858 [hep-ph]].
 - [7] A. Datta, K. Kong and K. T. Matchev, Phys. Rev. D **72**, 096006 (2005) [Erratum-ibid. D **72**, 119901 (2005)] [hep-ph/0509246].
 - [8] G. Servant and T. M. P. Tait, Nucl. Phys. B **650**, 391 (2003) [hep-ph/0206071].
 - [9] K. Kong and K. T. Matchev, JHEP **0601**, 038 (2006) [hep-ph/0509119].
 - [10] H. -C. Cheng, J. L. Feng and K. T. Matchev, Phys. Rev. Lett. **89**, 211301 (2002) [hep-ph/0207125].
 - [11] G. Servant and T. M. P. Tait, New J. Phys. **4**, 99 (2002) [hep-ph/0209262].
 - [12] P. A. R. Ade *et al.* [Planck Collaboration], arXiv:1303.5076 [astro-ph.CO].
 - [13] Z. Ahmed *et al.* [CDMS-II Collaboration], Science **327**, 1619 (2010) [arXiv:0912.3592 [astro-ph.CO]].
 - [14] E. Aprile *et al.* [XENON100 Collaboration], Phys. Rev. Lett. **109**, 181301 (2012) [arXiv:1207.5988 [astro-ph.CO]].
 - [15] E. Aprile [XENON1T Collaboration], arXiv:1206.6288 [astro-ph.IM].
 - [16] L. Baudis [DARWIN Consortium Collaboration], J. Phys. Conf. Ser. **375**, 012028 (2012) [arXiv:1201.2402 [astro-ph.IM]].
 - [17] L. Baudis, PoS IDM **2010**, 122 (2011) [arXiv:1012.4764 [astro-ph.IM]].
 - [18] E. Aprile *et al.* [XENON100 Collaboration], Phys. Rev. Lett. **111**, 021301 (2013) arXiv:1301.6620 [astro-ph.CO].
 - [19] M. Felizardo, T. A. Girard, T. Morlat, A. C. Fernandes, A. R. Ramos, J. G. Marques, A. Kling and J. Puibasset *et al.*, Phys. Rev. Lett. **108**, 201302 (2012) [arXiv:1106.3014 [astro-ph.CO]].
 - [20] E. Behnke *et al.* [COUPP Collaboration], Phys. Rev. D **86**, 052001 (2012) [arXiv:1204.3094 [astro-ph.CO]].